SUPPLEMENTARY FIGURES

MYC Overexpression Drives Immune Evasion in Hepatocellular Carcinoma (HCC) that is Reversible Through Restoration of Pro-Inflammatory Macrophages

Supplementary Figure 1 MYC gene amplifications in Human Cancers

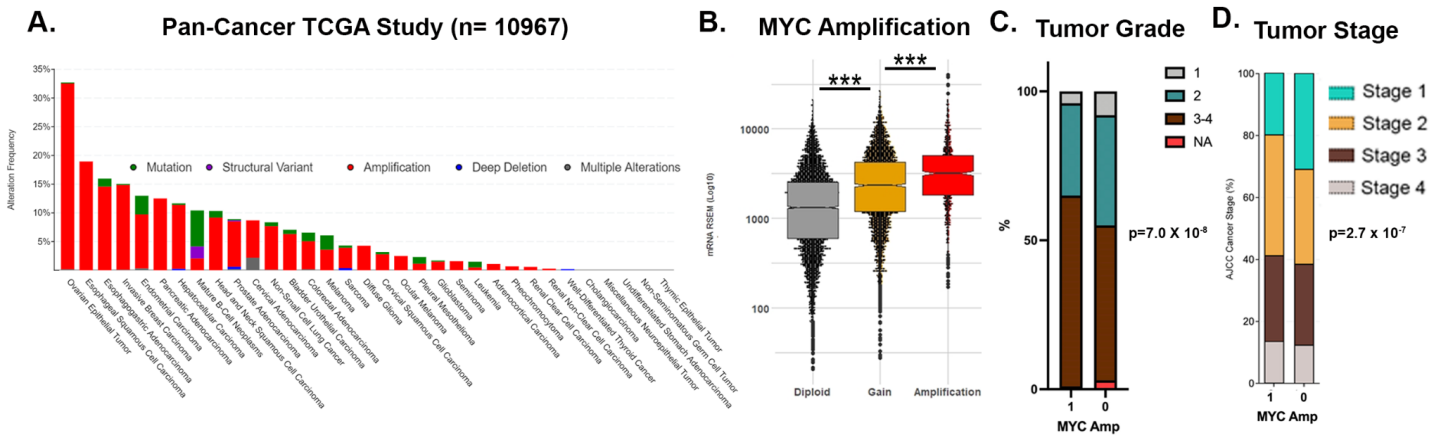

A. Prevalence of *MYC* gene amplifications across the 33 TCGA cancers.

B. MYC gene amplification strongly correlates with *MYC* mRNA expression across 33 cancers in the TCGA cohort.

C. Association of *MYC* amplification (1) in tumors with tumor grade across 33 cancers in the TCGA cohort.

D. Association of *MYC* amplification (1) in tumors with tumor stage across 33 cancers in the TCGA cohort.

Supplementary Figure 2 Immune Changes Associated with MYC Overexpression in Human Tumors

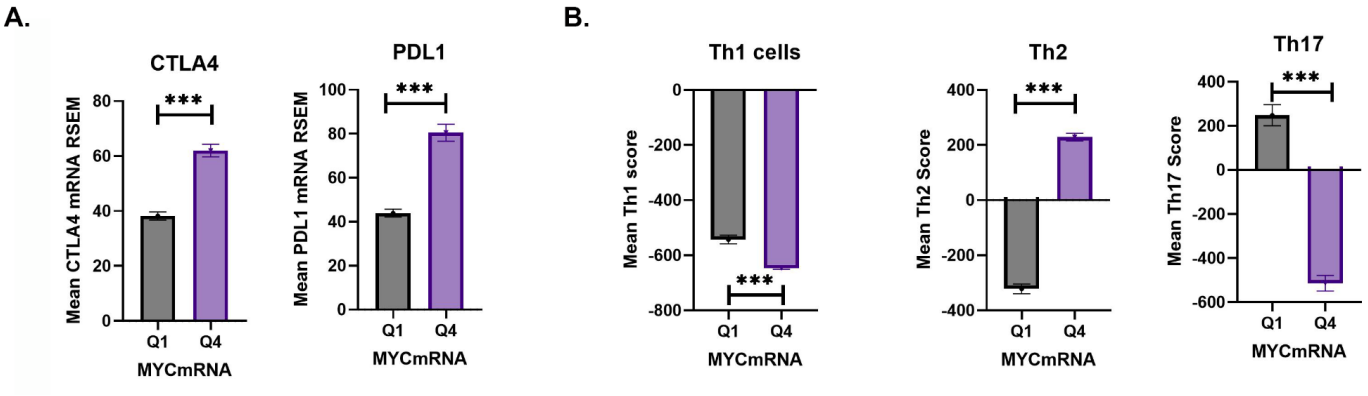

A. Highest quartiles of MYC expression are associated with higher levels of PDL1 and CTLA4 expression across 33 cancers in the TCGA cohort.

B. Highest quartiles of MYC expression are associated with lower Th1 expression, higher Th2 expression and lower Th17 immune signature expression scores across 33 cancers in the TCGA cohort.

Supplementary Figure 3 MYC mRNA and Protein Overexpression in Human Cancers.

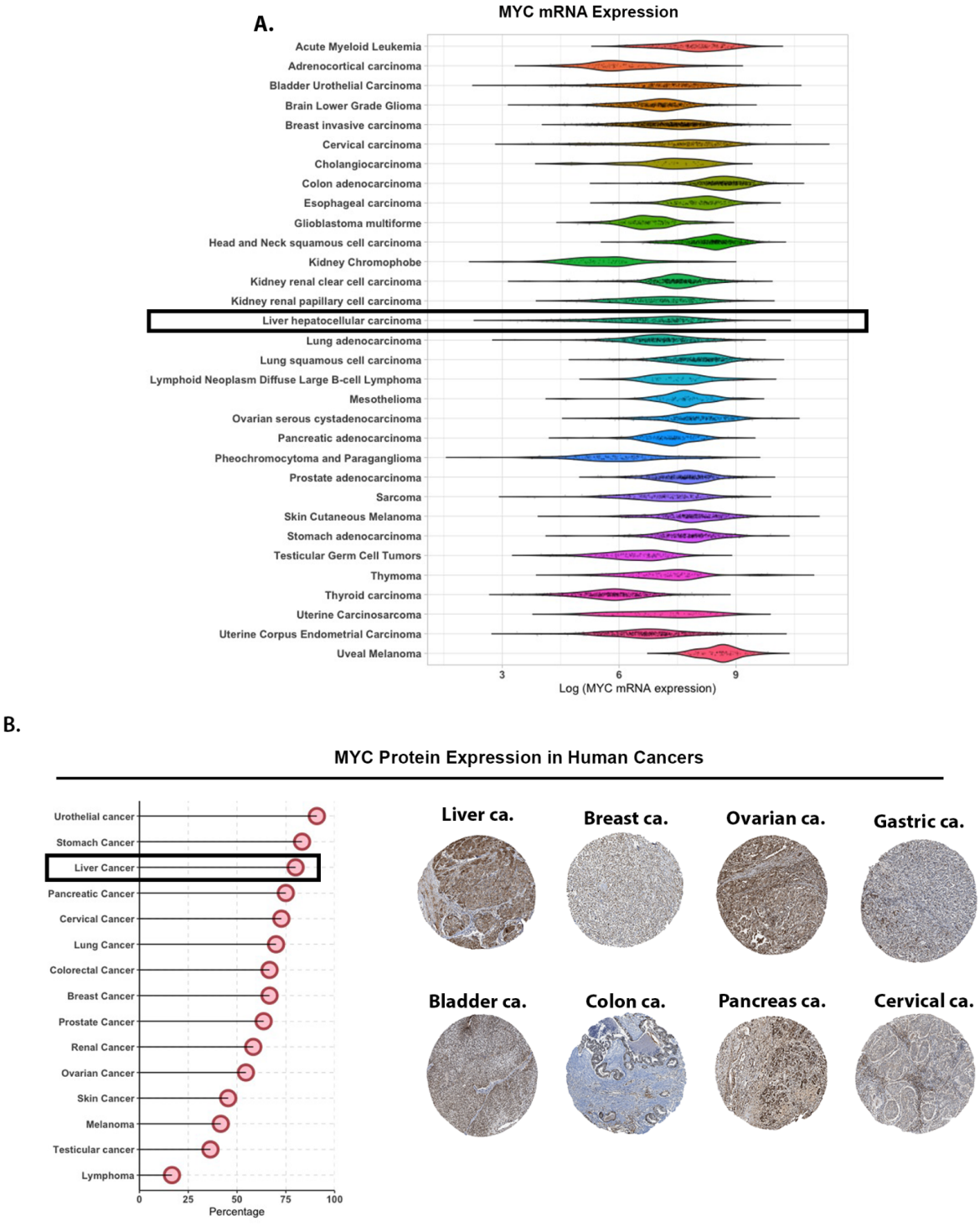

A. *MYC* gene mRNA expression across the 33 TCGA cancers.

B. Data from the Human Protein Atlas showing top 10 cancers with MYC protein overexpression (https://www.proteinatlas.org/ENSG00000136997-MYC/pathology).

Supplementary Figure 4 Pathways activated upon MYC inactivation in MYC-driven HCCs.

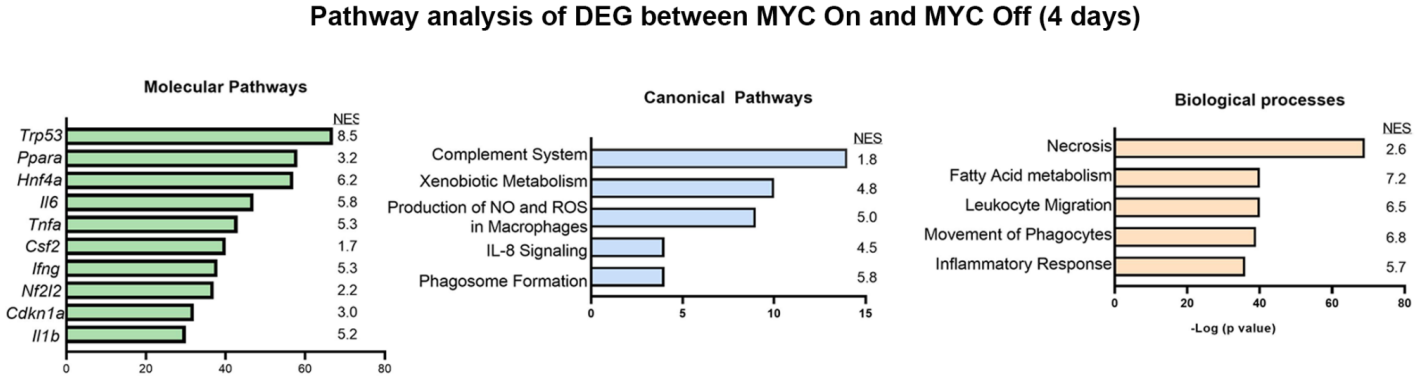

Top molecular pathways, canonical pathways and biological processes activated in murine MYC HCC (n=3) upon MYC inactivation for 4 days (n=3).

Supplementary Figure 5 Pathways activated with MYC mutant or short term MYC inactivation in HCCs.

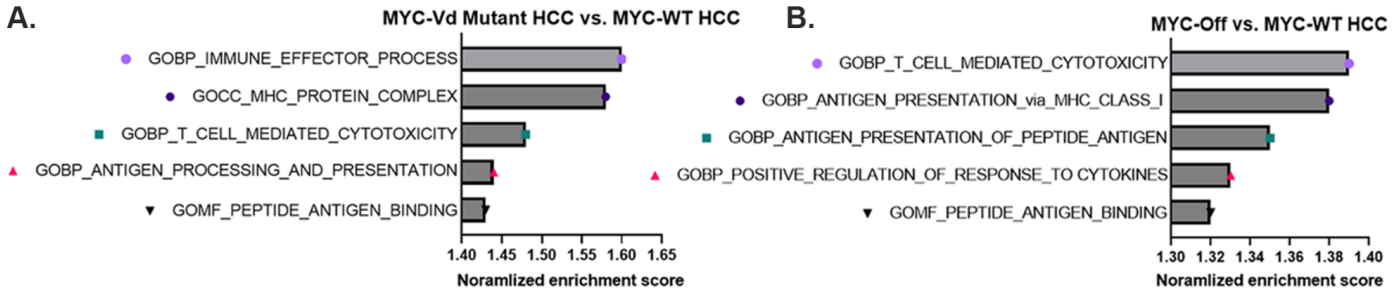

A. Top molecular pathways activated in murine MYC HCC overexpressing MYC Vd mutant (MYC^{Vd}, n=11) versus Wild Type MYC (n=16).

B. Top molecular pathways activated in murine MYC HCC upon 16-hr MYC inactivation (n=8) versus those expressing Wild Type MYC (n=16).

Supplementary Figure 6 Immune Checkpoint Inhibition Leads to Proliferative Arrest in MYC-HCC

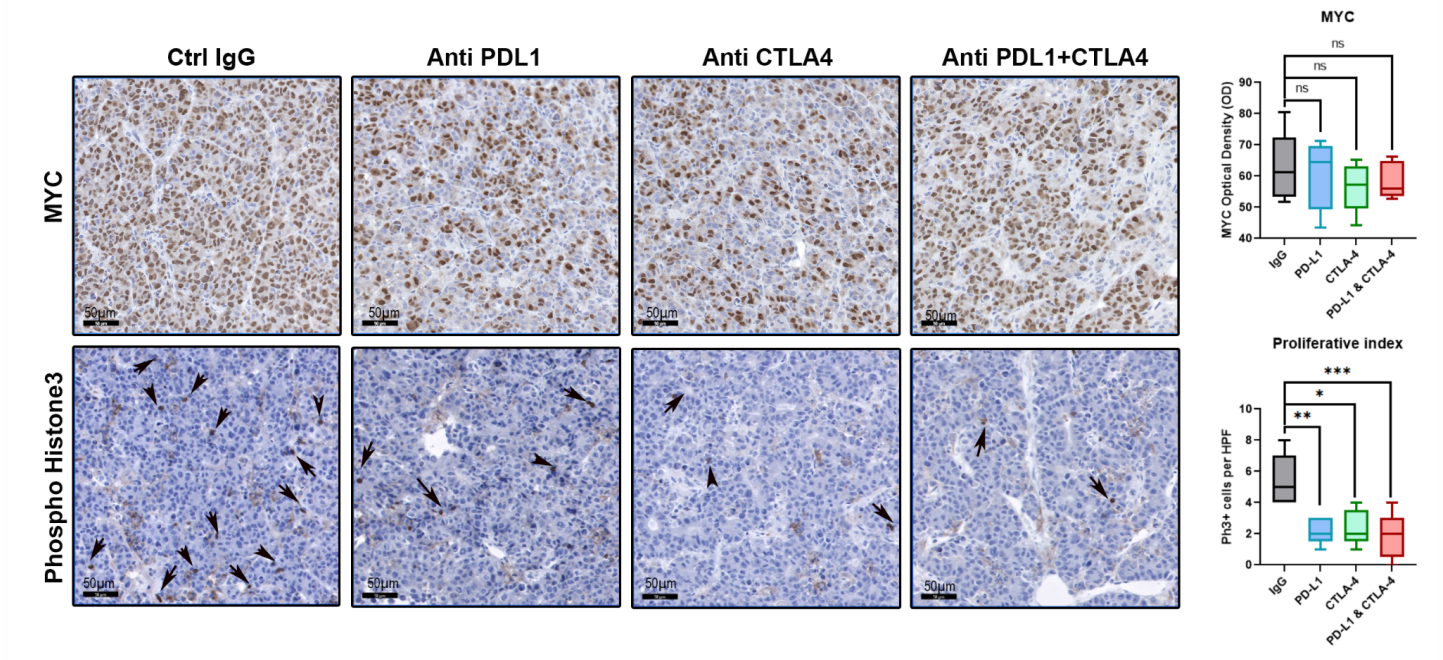

Immunohistochemistry showing MYC and phospho-histone 3 staining and quantification in MYC-HCC treated with IgG control (n=5), PDL1 antibody (n=5), CTLA4 antibody (n=5), or their combination.

Supplementary Figure 7 Immune Checkpoint Inhibition Leads to Cell Death in MYC-HCC

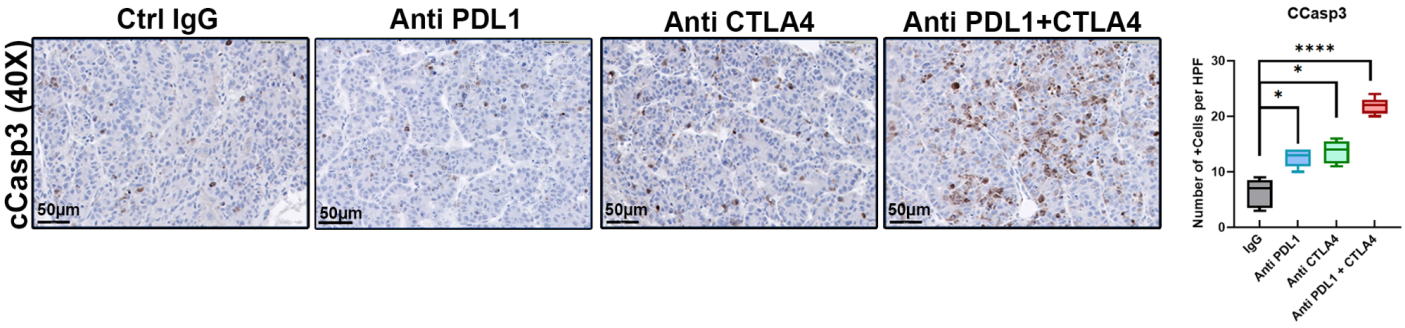

Immunohistochemistry showing cleaved caspase 3 staining and quantification in MYC-HCC treated with IgG control (n=5), PDL1 antibody (n=5), CTLA4 antibody (n=5), or their combination.

Supplementary Figure 8 Macrophage repolarization with combination Immune Checkpoint inhibition in MYC-HCC

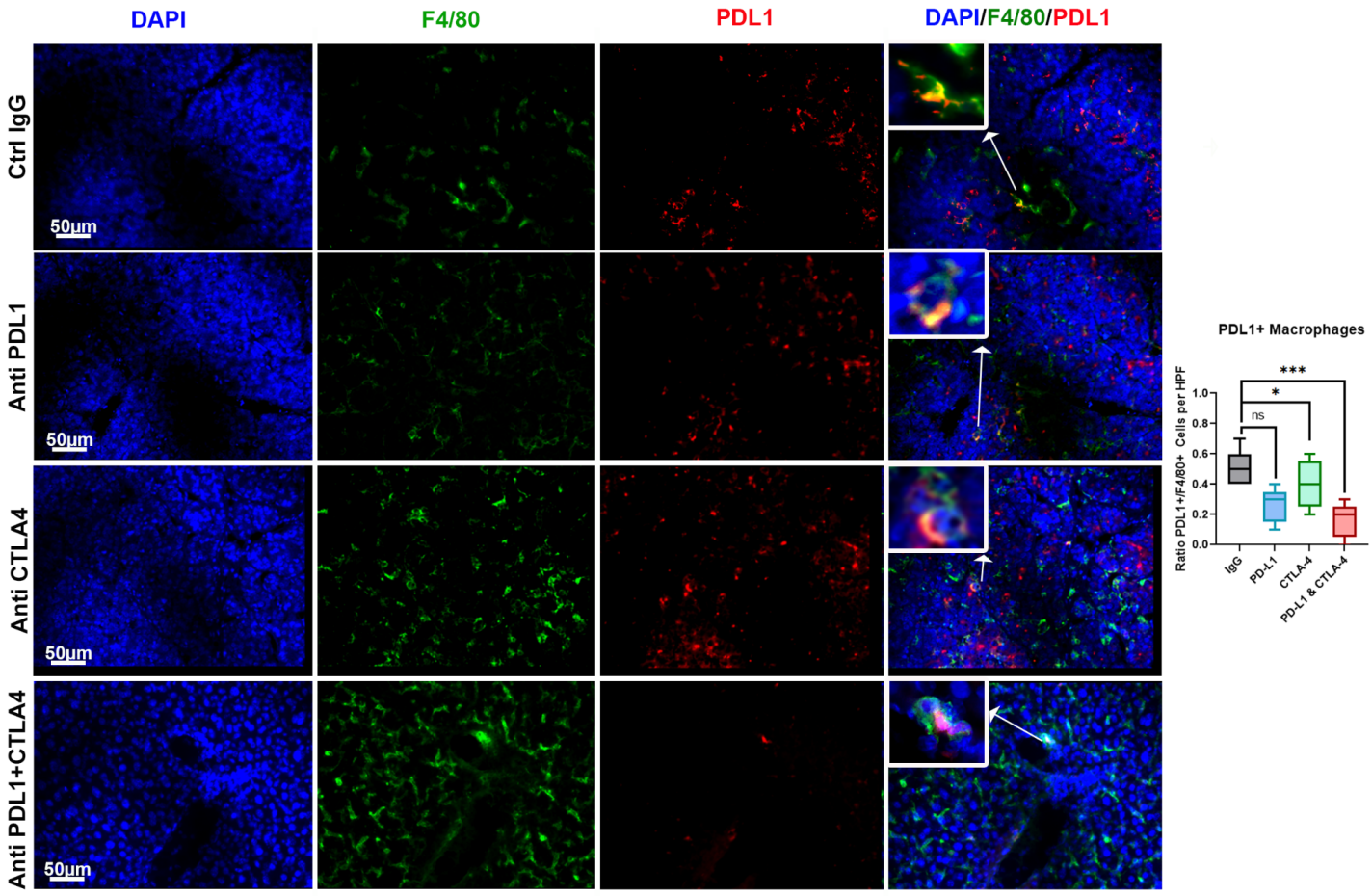

Immunofluorescence showing PDL1 and F4/80 double staining and quantification in MYC-HCC treated with IgG control (n=5), PDL1 antibody (n=5), CTLA4 antibody (n=5), or their combination (n=5).

Supplementary Figure 9 Transcriptomic changes induced by immunotherapy in MYC-HCC

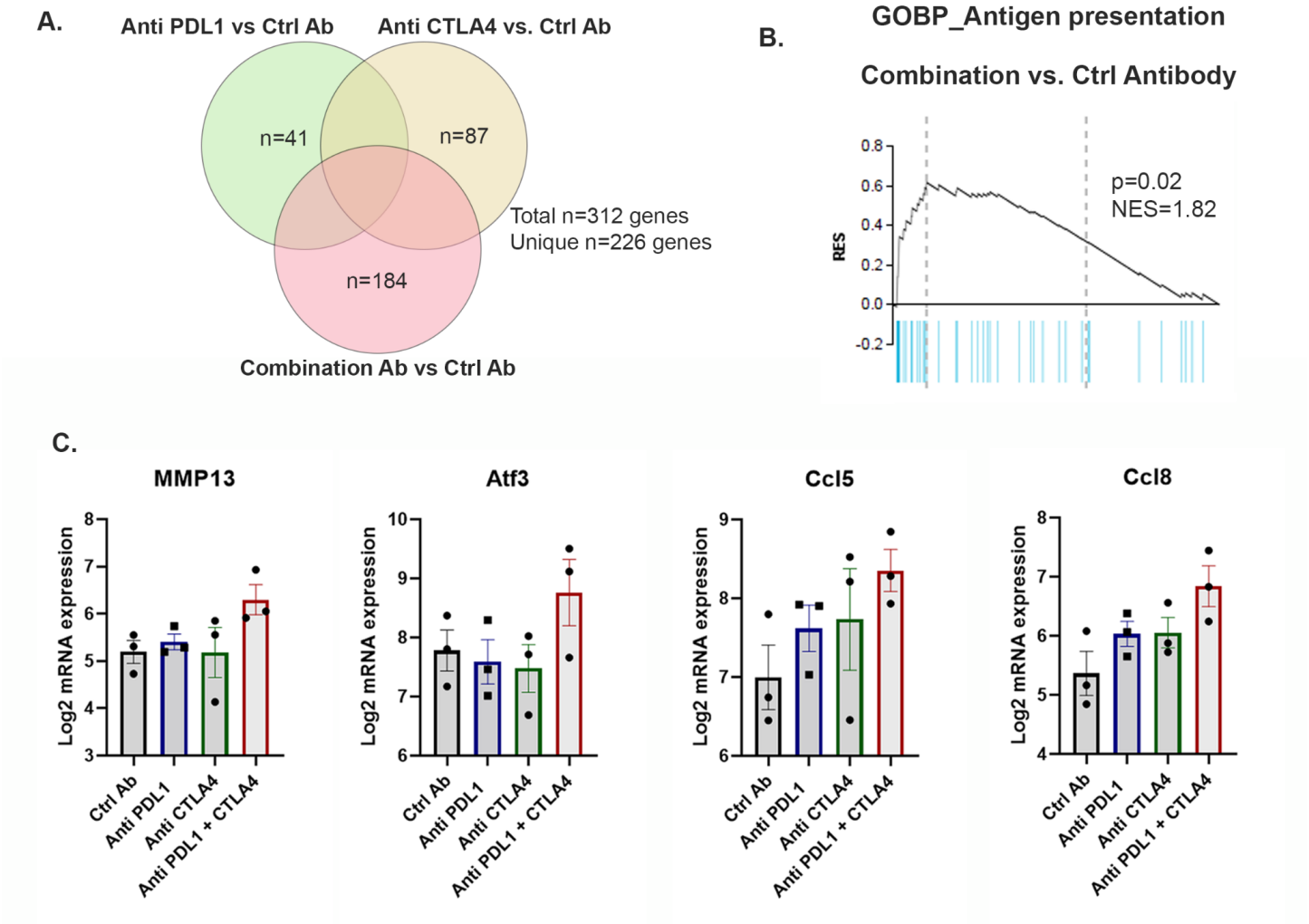

A. Venn diagram showing the meta-analysis of the three different comparisons between tumors treated with anti PDL1 antibody alone (n=3), anti CTLA4 ab (n=3, combination of anti PDL1 and CTLA4 antibodies (n=3) or control IgG antibody (n=3).

B. Enrichment of antigen presentation pathway in tumors treated with combination of anti PDL1 and CTLA4 antibodies (n=3) versus control IgG antibody (n=3).

C. Specific macrophage related genes that are upregulated in tumors treated with combination of anti PDL1 and CTLA4 antibodies (n=3) versus anti PDL1 (n=3) or anti CTLA 4 (n=3) monotherapies or control IgG antibody (n=3).

Supplementary Figure 10 Mass Cytometry Analysis of Immune Response to Immune Checkpoint Inhibitors in MYC-HCC

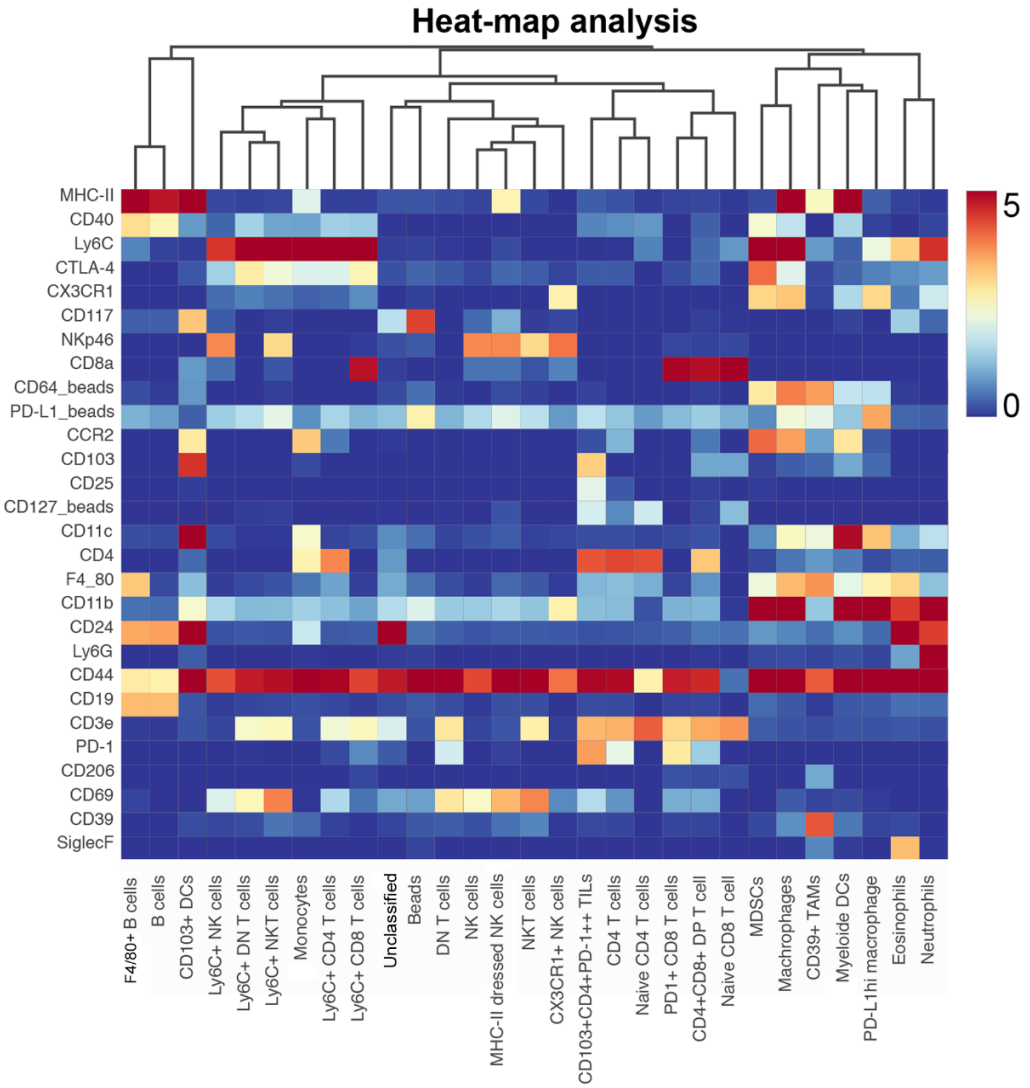

Heatmap shows expression of different immune markers in the identified immune subsets from the mass cytometry analysis of MYC-HCC treated with IgG control (n=3), PDL1 antibody (n=3), CTLA4 antibody (n=2), or their combination (n=4).

Supplementary Figure 11 Inflammatory macrophages increase with combination immunotherapy of MYC-HCC

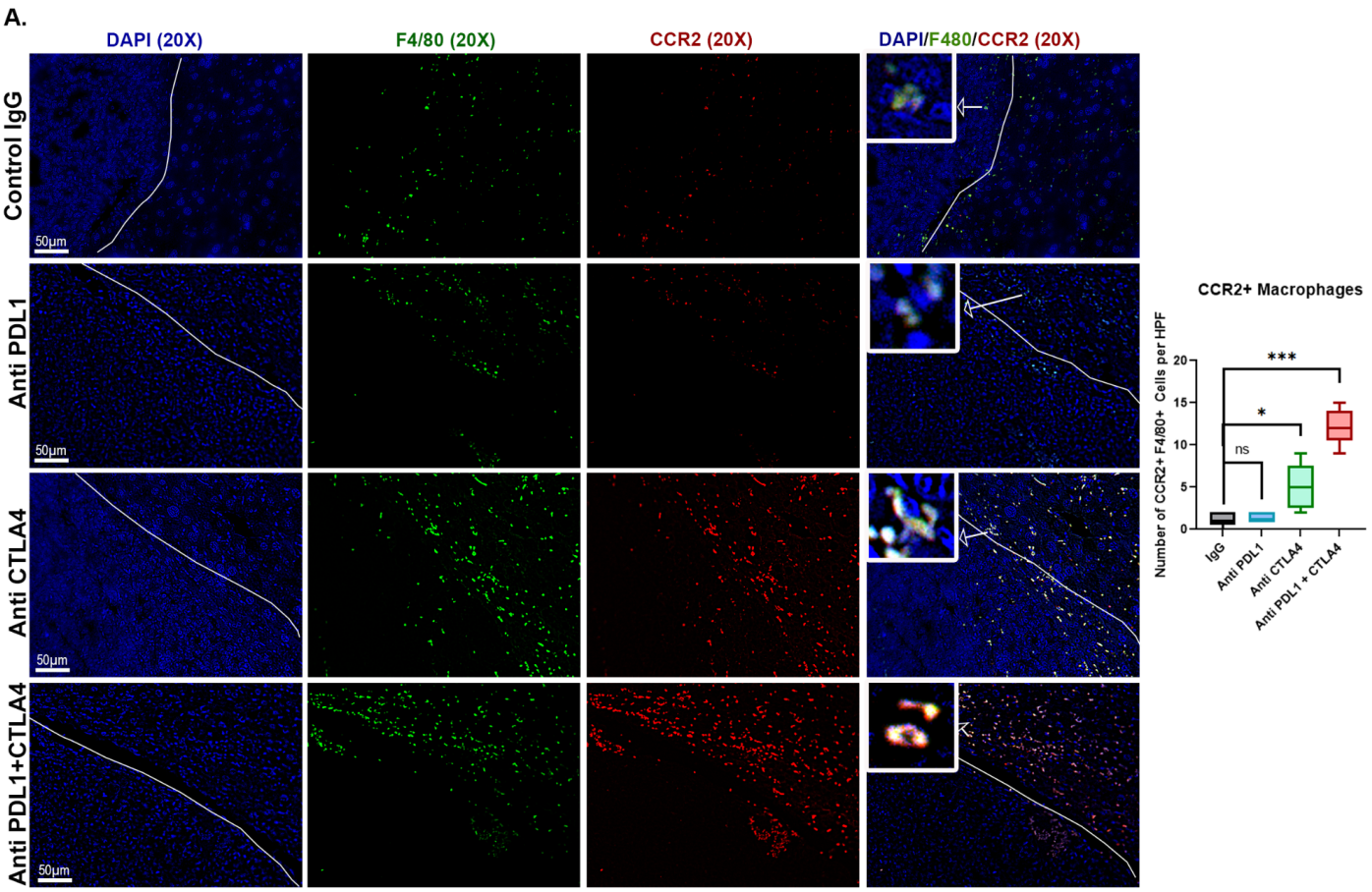

Immunofluorescence showing CCR2 and F4/80 double staining and quantification in MYC-HCC treated with IgG control (n=3), PDL1 antibody (n=3), CTLA4 antibody (n=3), or their combination (n=3).

Supplementary Figure 12 M2-like macrophages decrease with combination immunotherapy of MYC-HCC

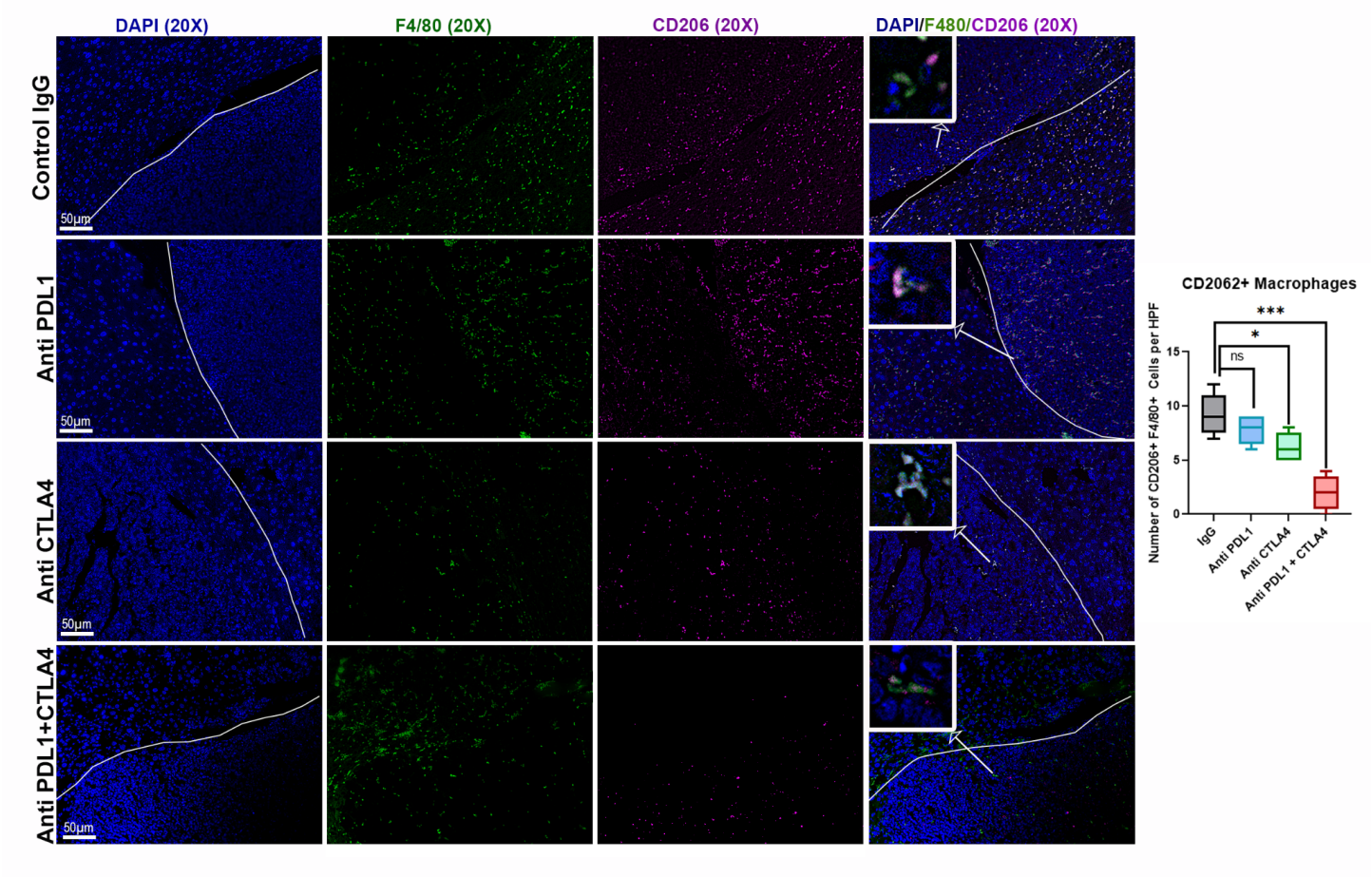

Immunofluorescence showing CD206 and F4/80 double staining and quantification in MYC-HCC treated with IgG control (n=3), PDL1 antibody (n=3), CTLA4 antibody (n=3), or their combination (n=3).

Supplementary Figure 13 No change in other Major Immune Subsets between the treatment groups

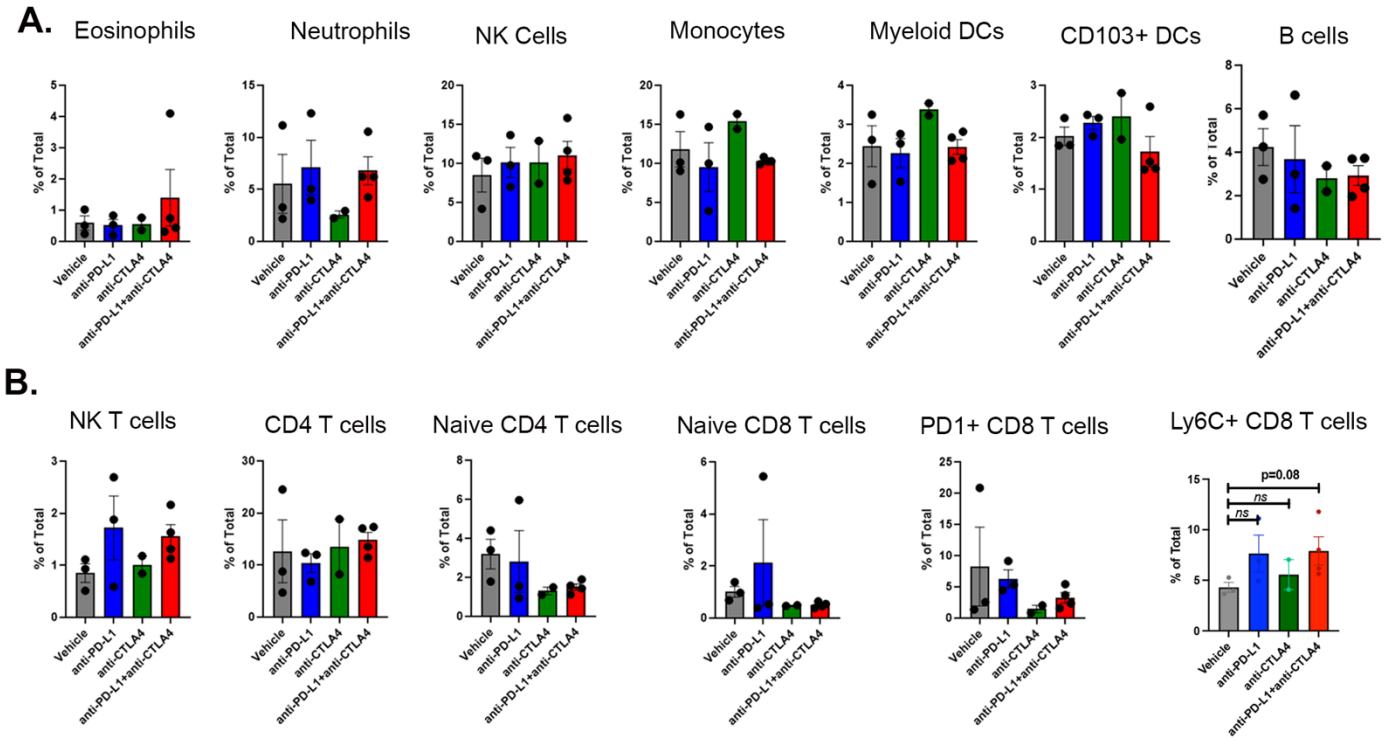

A and B. Comparison of abundance of multiple immune subsets on mass cytometry analysis in MYC-HCC treated with IgG control, PDL1 antibody, CTLA4 antibody, or their combination.

Supplementary Figure 14 Anti CSF1R Treatment in MYC-HCC

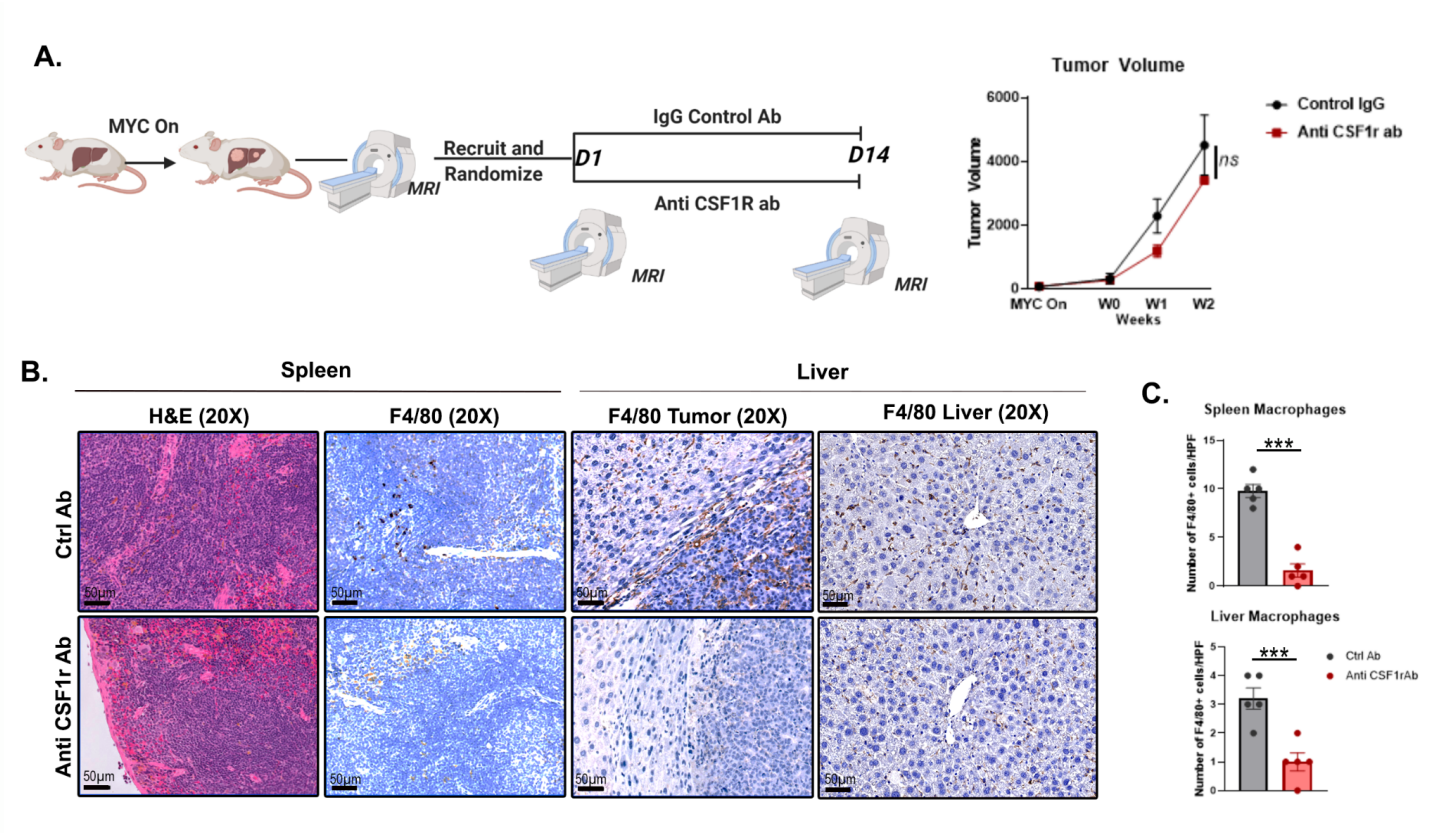

A. Experimental scheme of MYC-HCC mice treated with anti CSF1R antibody (n=4) or control antibody (n=4). No difference in tumor progression was noted on MRI volumetric tumor measurement.

B. Representative images of spleen and IHC for F4/80 confirming macrophage depletion with anti CSF1R antibody both in the spleen and the tumor and non-tumorous liver.

C. Quantification of splenic and liver macrophages in CSF1R antibody-treated MYC-HCC mice compared to control antibody treated mice.